

PAPER • OPEN ACCESS

## Study on the effect of displacement fluid viscosity on the microscale residual oil saturation and characteristics

To cite this article: Zhangpeng Hu *et al* 2021 *J. Phys.: Conf. Ser.* **2044** 012026

View the [article online](#) for updates and enhancements.

You may also like

- [Experimental Study and Numerical Simulation on Residual Welding Stress Relaxation](#)  
Min Wang, Weilian Qu and Yifei Wang
- [Research on the Hydrodynamics of the Mechanism of Viscous-Elastic Fluids Displacing Residual Oil Droplets in Micro Pores](#)  
Guiling Chen
- [Effect of the Leveling Conditions on Residual Stress Evolution of Hot Rolled High Strength Steels for Cold Forming](#)  
Keecheol Park and Kyungsuk Oh



**ECS**  
The  
Electrochemical  
Society  
Advancing solid state &  
electrochemical science & technology

**DISCOVER**  
how sustainability  
intersects with  
electrochemistry & solid  
state science research

# Study on the effect of displacement fluid viscosity on the microscale residual oil saturation and characteristics

Zhangpeng Hu<sup>1</sup>, Haonan Fang<sup>1</sup>, Jing Yang<sup>1</sup>, Yafei Liu<sup>1,\*</sup>

<sup>1</sup>Department of Petroleum Engineering, Xi'an Shiyou University, Xi'an, Shaanxi, China

\* Correspondence: yafliu@xsyu.edu.cn

**Abstract** Waterflooding is regarded as one of the most common methods for oil recovery yet a great portion of residual oil still remained in the reservoir after waterflooding. Therefore, investigation on the residual oil saturation and its characteristics is of great importance. Specifically, microscale residual oil pattern and saturation are crucial to the analysis of oil recovery efficiency and decision for future EOR methods. In this work, transparent microfluidic devices were adopted to simulate waterflooding process and observe the change in the oil saturation as well as the residual oil pattern. Meanwhile the impact of displacement fluid viscosity and displacement rate on the residual oil saturation and pattern was inspected. Results revealed that as the displacement fluid viscosity increased from 0.895 to 1.763mPa·s, residual oil saturation decreased from 31.2 to 20%. Three patterns of residual oil were observed which were bulk, columnar and dead-end respectively. Bulk pattern took up the largest portion of the total residual oil, and as the displacement fluid viscosity increasing, decrease in the bulk oil saturation was the greatest. Dead-end residual oil contributed the least to the oil recovery and it could be the potential target for the future EOR method.

## 1. Introduction

Waterflooding has been widely applied worldwide for oil recovery owing to its low-cost and convenient features. However there still exists large quantity of residual oil after waterflooding process. Therefore, study on the distribution and characteristics of residual oil has long been the focus in order to choose the appropriate EOR methods and reduce the residual oil saturation[1-3]. Studies have shown that various factors could impact the residual oil saturation including pore throat structure, wettability, mobility ratio and injected fluid chemistry properties[4-6].

Residual oil has been investigated in both macro and micro scales via different methods including reservoir simulation, core flooding, NMR and CT scanning, and micromodels to study the residual oil distribution, quantity and characteristics[3-5,7]. Core flooding tests utilize core samples to simulate different flooding methods and obtain the corresponding oil recovery potential, however fluid distribution inside the cores could be difficult to observe. To compensate for that NMR and CT scanning are usually combined with core flooding tests to acquire both macro scale oil recovery and microscale oil and water distribution[8]. These scanning technologies enabled the tracking of oil and water distribution within a real rock sample yet visualization of dynamic interactions between oil and water during waterflooding are still difficult to accomplish. Therefore, microfluidic devices have been employed in order to further examine the dynamic pore-scale residual oil change and its characteristics.

Microfluidics emerged decades ago[9] and microfluidic devices could be fabricated with silicon [10], glass [11], polymers like polydimethylsiloxane (PDMS)[12], among which PDMS devices are cheap



and convenient to duplicate such that a fresh and identical device could be used for each experiment to ensure the consistency of the initial experiment state [13]. Therefore, in this work, microfluidic devices were employed to examine the residual oil saturation and its microscale characteristics after waterflooding process. The influence of displacement fluid viscosity and displacement speed on the residual oil was also incorporated.

## 2. Material & Methods

### 2.1 Materials

Microfluidic devices with realistic pore-throat topology were used to investigate the micro-scale residual oil saturation and characteristics. Devices were fabricated using polydimethylsiloxane (PDMS) via typical photolithography and soft lithography approach. Mineral oil was used as the oil phase. In order to examine the effect of displacement fluid viscosity on the residual oil saturation after waterflooding, aqueous solutions with varying viscosity were prepared by adding 0, 10, 20, 30 and 40wt% glycerol solution to deionized (DI) water. Furthermore, 0.1wt% Rhodamine B was added to the aqueous phase to differentiate between mineral oil and aqueous solution. The viscosity of all the fluids were measured and listed in the table below.

Table 1. Summary of the fluid viscosity

	Aqueous phase					Oil phase
	0% glycerol	10% glycerol	20% glycerol	30% glycerol	40% glycerol	
Viscosity (mPa·s)	0.895	0.984	1.223	1.480	1.763	21.25

### 2.2 Methods

Experimental apparatus used in this work were inverted microscope, syringe pumps and high speed camera connected to a computer. 1mL syringes connected with Teflon tubing were filled with oil and dyed DI water respectively and installed in the syringe pump. Firstly, DI water was injected into the microfluidic device at the rate of 5 $\mu$ L/min until the saturation no longer changed in order to establish the initial water saturation. Then mineral oil was injected at the same rate to displace the indigenous water until the oil saturation no longer changed and establish the initial oil saturation. Afterwards waterflooding process was simulated by injecting DI water with certain viscosity at the rate of 0.5 $\mu$ L/min to begin with. Dynamic interactions between oil and water were observed through the microscope and captured via the high speed camera. Images were captured average one second until the residual oil saturation stabilized. At this point the injection rate was increased to 0.8 $\mu$ L/min to further improve the oil recovery and examine the influence of injection rate on the residual oil saturation. Waterflooding process ceased when the residual oil saturation stayed the same. Images were captured throughout the whole process and the aforementioned experimental procedures were repeated with varying aqueous phase viscosity.

## 3. Results and Discussion

### 3.1 Image process

To investigate the influence of displacement fluid viscosity on the residual oil saturation, the captured images during the experiment were analyzed via ImageJ software. Rock matrix and fluids were distinguished to obtain the porosity of the microfluidic device which was 57%. As shown in Figure 1, dyed fluid was the aqueous phase and it was differentiated from the oil phase after processing the image. Its area fraction was calculated using ImageJ such that residual oil saturation for each captured image was obtained via the following equation.

$$\text{Residual oil saturation} = \frac{\text{Device porosity} - \text{area fraction of the aqueous phase}}{\text{Initial oil saturation}} \times 100\%$$

The pore volume (PV) of the microfluidic device was  $0.524\mu\text{L}$ ; combined with the displacement rate and image capture rate, the relationship between number of PV fluid injection and residual oil saturation could be derived.

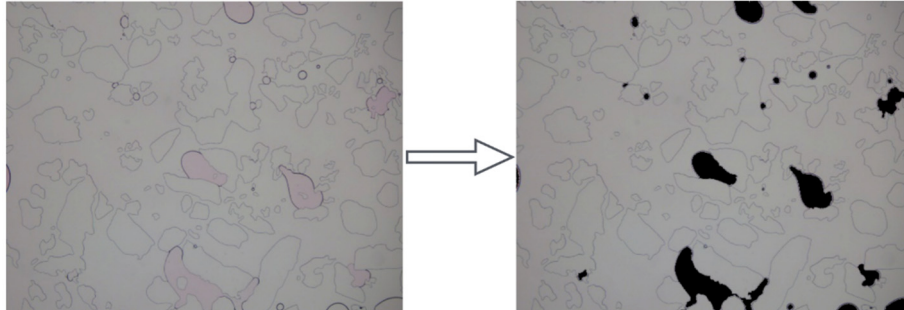


Figure 1. Illustration of the image process

### 3.2 Displacement fluid viscosity versus residual oil saturation

In this work, five aqueous solutions with different viscosity were applied as the displacement fluid during the waterflooding process. Residual oil saturation after each waterflooding was demonstrated in Figure 2. Overall the residual oil saturation decreased as the displacement fluid viscosity increased. The residual oil saturation decreased from 36.9% to 27.7% when the displacement fluid viscosity doubled demonstrating the influence of fluid viscosity or mobility ratio on the oil recovery on the macro-scale. This plot also incorporates the residual oil saturation change as the displacement rate increased from 0.5 to  $0.8\mu\text{L}/\text{min}$ . Intuitively residual oil saturation reduced as the displacement rate increased. Moreover, the reduction of residual oil saturation was greater when the displacement fluid viscosity was higher.

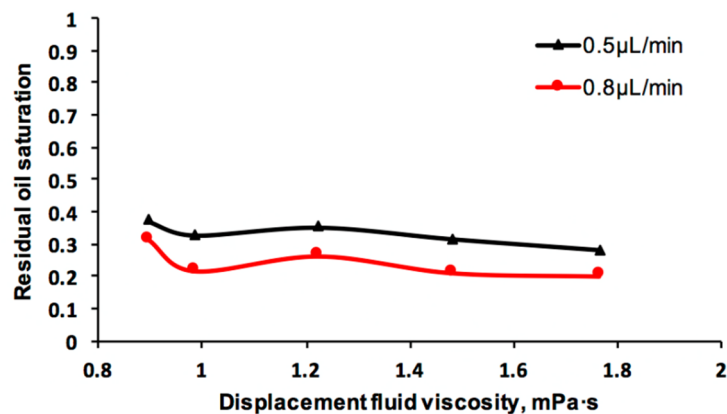


Figure 2. Residual oil saturation versus different displacement fluid viscosity at two displacement rates

Dynamic residual oil saturation was recorded during the whole waterflooding process. Figure 3 plotted the number of PV fluid injected versus the corresponding residual oil saturation as the displacement fluid viscosity varied. It was observed that at the beginning of waterflooding oil saturation reduced rapidly presumably larger pores were quickly occupied. The curve gradually flattened out after approximately 1.28PV of aqueous solution injected. It was also observed that the reduction rate of oil saturation was almost the same for the five curves indicating displacement fluid viscosity has smaller impact on the displacement rate. After injecting almost 6.08PV fluid, the displacement rate was increased to  $0.8\mu\text{L}/\text{min}$ . As shown in Figure 3, a slight and gentle decrease in oil saturation occurred and at 7.04PV the curve gradually reached the plateau. The difference among the five curves was more distinct compared with the first half suggesting displacement fluid viscosity has greater influence on the oil saturation when the displacement rate was higher and after majority of the mobile oil has been recovered. Waterflooding finally ceased when 12.8PV fluid was injected.

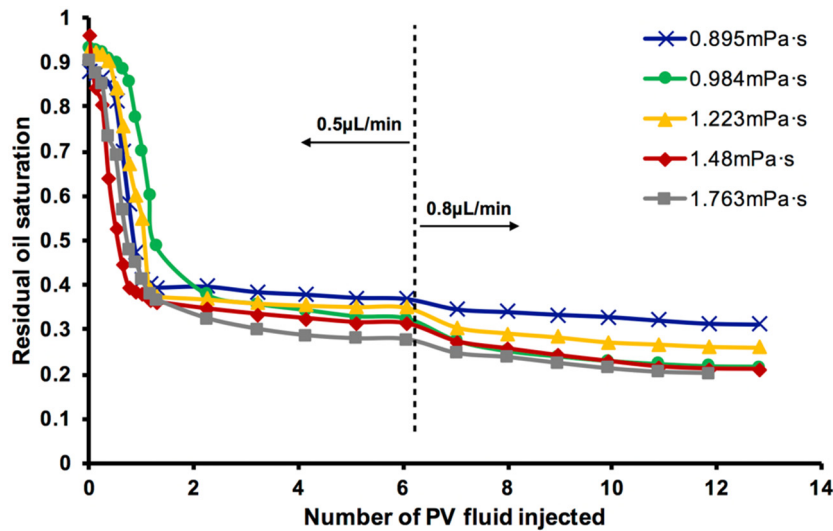


Figure 3. Relationship between the oil saturation and the number of PV displacement fluid injected for five viscosity scenarios

3.3 Characteristics of microscale residual oil pattern

Macroscale residual oil saturation is comprised of microscale oil clusters and the investigation on the microscale residual oil pattern could be beneficial to the analysis of oil recovery and the application of EOR process. Therefore, in this work, pore scale residual oil characteristics was inspected via the images taken during the experiment. The pattern of the observed residual oil was approximately categorized as bulk, columnar and dead-end and was shown in Figure 4. Bulk residual oil mostly existed in larger pores and took up larger portion of the total residual oil. Columnar residual oil usually existed within throats and resembled columns. Dead-end residual oil was commonly trapped in the corners that partial oil was in contact with the rock matrix and partial oil was open to the pore space.

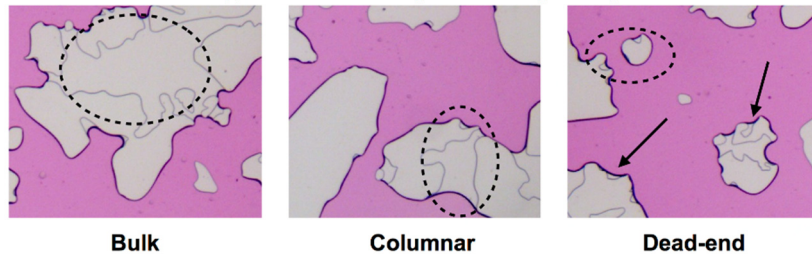


Figure 4. Demonstration of representative residual oil patterns with dashed circles and arrows

The portion of three different residual oil patterns was further quantified and results were demonstrated in Figure 5. Generally, the proportions of all three patterns decreased as the displacement fluid viscosity increased yet the reduction degree varied. When the displacement rate was 0.5 μL/min, bulk residual oil proportion was 25.3%, 22.4%, 23.7%, 21.6% and 19.4% respectively as fluid viscosity increased. Columnar residual oil proportion was 7.1%, 6.1%, 6.9%, 5.4% and 5.2% respectively as fluid viscosity increased. Dead-end residual oil proportion was 4.5%, 3.9%, 4.3%, 4.2% and 3.1% respectively as fluid viscosity increased. When the displacement rate was 0.8 μL/min, bulk residual oil proportion was 18.2%, 12.4%, 15.6%, 11.5% and 10.8% respectively as fluid viscosity increased. Columnar residual oil proportion was 8.2%, 5.9%, 6.7%, 5.9% and 5.6% respectively as fluid viscosity increased. Dead-end residual oil proportion was 4.8%, 3.3%, 3.7%, 3.6% and 3.6% respectively as fluid viscosity increased. It was observed that bulk residual oil largely contributed to the total residual oil reduction and the increase in fluid viscosity has relatively greater impact on bulk and columnar residual oil. As for the recovery of dead-end crude oil, EOR methods like surfactant flooding and polymer flooding might be effective.

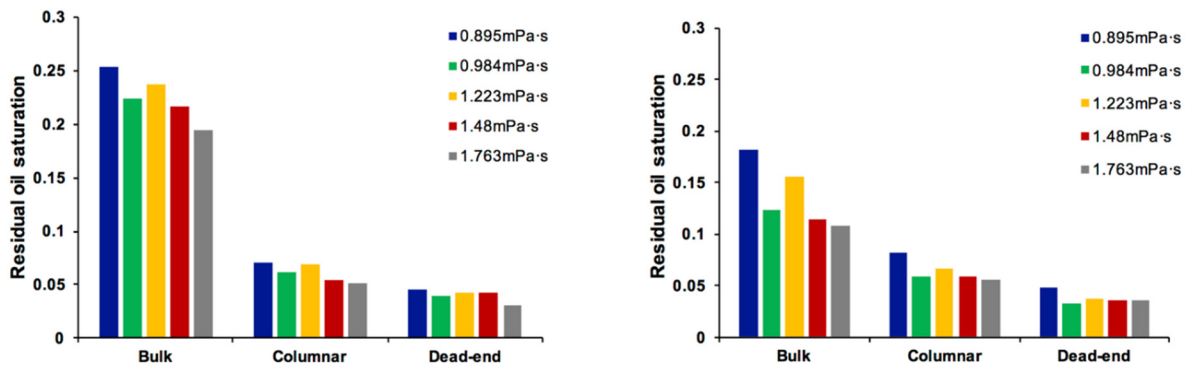


Figure 5. Demonstration on the proportion of three residual oil patterns after waterflooding with varying displacement fluid viscosity

#### 4. Conclusions

In this work the influence of displacement fluid viscosity on the oil recovery and microscale residual oil saturation was examined. Waterflooding process was simulated using microfluidic devices during which images were captured for further analysis. Two displacement rate were applied to further investigate its effect on the residual oil saturation. When the aqueous phase viscosity increased from 0.895 to 1.763 mPa·s, residual oil saturation decreased from 31.2 to 20% which was owing to the improvement of displacement phase mobility. Intuitively residual oil saturation reduced as the displacement rate increased. The reduction of residual oil saturation was greater when the displacement fluid viscosity was higher. The observed patterns of microscale residual oil after waterflooding in this work were categorized as bulk, columnar and dead-end; among which bulk residual oil took up the largest portion followed by columnar residual oil. As the viscosity of the water phase increases, the decrease in oil saturation mainly comes from bulk residual oil. Dead-end residual oil contributed the least and it was considered as the potential target for the future EOR method.

#### Acknowledgments

This work was financially supported by the National Natural Science Foundation of China (Grant No. 51904244 and 51934005).

#### References

- [1] Chatzis I, Morrow NR, Lim HT. Magnitude and Detailed Structure of Residual Oil Saturation. *Society of Petroleum Engineers Journal* 1983;23:311–26. doi:10.2118/10681-PA.
- [2] Erincik MZ, Qi P, Balhoff MT, Pope GA. New method to reduce residual oil saturation by polymer flooding. *SPE Journal* 2018;23:1944–56.
- [3] Guo Y, Zhang L, Zhu G, Yao J, Sun H, Song W, et al. A pore-scale investigation of residual oil distributions and enhanced oil recovery methods. *Energies* 2019;12:3732.
- [4] Shabaninejad M, Middleton J, Latham S, Fogden A. Pore-scale analysis of residual oil in a reservoir sandstone and its dependence on water flood salinity, oil composition, and local mineralogy. *Energy Fuels* 2017;31:13221–32.
- [5] Li J, Gao Y, Jiang H, Liu Y, Dong H. Pore-Scale Imaging of the Oil Cluster Dynamic during Drainage and Imbibition Using In Situ X-Ray Microtomography. *Geofluids* 2018;2018:1–13. doi:10.1155/2018/7679607.
- [6] Mehmani A, Kelly S, Torres-Verdín C, Balhoff M. Residual oil saturation following gas injection in sandstones: Microfluidic quantification of the impact of pore-scale surface roughness. *Fuel* 2019;251:147–61.
- [7] Xu K, Liang T, Zhu P, Qi P, Lu J, Huh C, et al. A 2.5-D glass micromodel for investigation of multi-phase flow in porous media. *Lab Chip* 2017;17:640–6. doi:10.1039/c6lc01476c.

- [8] Song R, Peng J, Sun S, Wang Y, Cui M, Liu J. Visualized experiments on residual oil classification and its influencing factors in waterflooding using micro-computed tomography. *Journal of Energy Resources Technology* 2020;142:083003.
- [9] Whitesides GM. The origins and the future of microfluidics. *Nature* 2006;442:368–73. doi:10.1038/nature05058.
- [10] Kovscek AR, Tang GQ, Radke CJ. Verification of Roof snap off as a foam-generation mechanism in porous media at steady state. *Colloids and Surfaces a: Physicochemical and Engineering Aspects* 2007;302:251–60. doi:10.1016/j.colsurfa.2007.02.035.
- [11] Liu Y, Block E, Squier J, Oakey J. Investigating low salinity waterflooding via glass micromodels with triangular pore-throat architectures. *Fuel* 2021;283:119264. doi:10.1016/j.fuel.2020.119264.
- [12] Duffy DC, McDonald JC, Schueller OJ, Whitesides GM. Rapid Prototyping of Microfluidic Systems in Poly(dimethylsiloxane). *Anal Chem* 1998;70:4974–84. doi:10.1021/ac980656z.
- [13] Quake SR, Scherer A. From micro- to nanofabrication with soft materials. *Science* 2000;290:1536–40. doi:10.1126/science.290.5496.1536.